

# Mechanical domain coupled mode parametric resonance and amplification in a torsional mode micro electro mechanical oscillator

Rajashree Baskaran and Kimberly L Turner

2355, Engr II, Department of Mechanical Engineering, University of California, Santa Barbara, CA 93105, USA

E-mail: raji@engineering.ucsb.edu.

Received 9 January 2003, in final form 7 May 2003

Published 20 June 2003

Online at [stacks.iop.org/JMM/13/701](http://stacks.iop.org/JMM/13/701)

## Abstract

In this paper, we experimentally demonstrate non-degenerate parametric resonance in a torsional micro electro mechanical (MEM) oscillator with two interacting mechanical modes of oscillation. The parametric oscillation results from a displacement-dependent electrostatic force generated in both the modes of oscillation. There is a decoupling of the input and the output frequencies in this mode of operation where the system responds at the primary natural frequency when driven at the sum of the first two mechanical modes. This can be implemented in many commonly used MEM oscillator configurations including the cantilever beam geometry. In this mode of operation, single oscillator non-degenerate parametric amplifiers as well as resonant mode sensors based on the frequency selectivity of parametric resonance can be implemented.

## 1. Introduction

Resonant mode operation of micro electro mechanical (MEM) oscillators has many applications which include sensing, on-chip filters/switches/mixers in the radio frequencies [1], scanning probe microscopy [2, 3] and small force detection [4]. When operated in the linear regime as simple harmonic oscillators (SHO), there exists a tradeoff between the selectivity (quality factor) and the bandwidth of operation. Also, the selectivity (quality factor) is primarily controlled by viscous damping which depends on the ambient working conditions and cannot be controlled in open loop implementation. Some of these issues can be overcome by operating in parametric sub-harmonic resonance if the effective stiffness of the oscillator can be made time dependent. In voltage-controlled electrostatic actuation, the force generated is proportional to the square of the voltage and this implies the frequency of forcing will be double the driving voltage frequency for dynamic forcing ( $F_e = k_e V^2 = k_e [\cos(\omega t)]^2 = k_e [1 + \cos(2\omega t)]/2$ ). This nonlinear electro-mechanical transduction could be used conveniently, with suitable design, to excite the first parametric

sub-harmonic resonance (at half the driving frequency) whereby the overall system input and output frequencies will remain the same.

In this paper, we present experimental results of operation of a single oscillator with time varying stiffness (due to electrostatic actuation) as an auto-parametric amplifier in both degenerate and non-degenerate modes. In the context of this paper, degenerate parametric amplification refers to a gain in motion amplitude due to the presence of a 'pump' parametric (displacement-dependent) force at twice the response frequency and non-degenerate amplification refers to the gain in motion amplitude when the 'pump' is at the sum of the two frequencies [5]. While there is previous work regarding degenerate parametric amplification or resonance in single MEM oscillators [6–8] and non-degenerate amplification using nonlinear mechanical stiffness [9, 10] or in coupled two oscillator systems [11, 12], this study presents parametric coupling between two distinct mechanical modes in a single electrostatic MEM oscillator (non-degenerate parametric amplification). The stiffness corresponding to the first two natural modes of this oscillator can be time dependent and under such a condition the 'sum

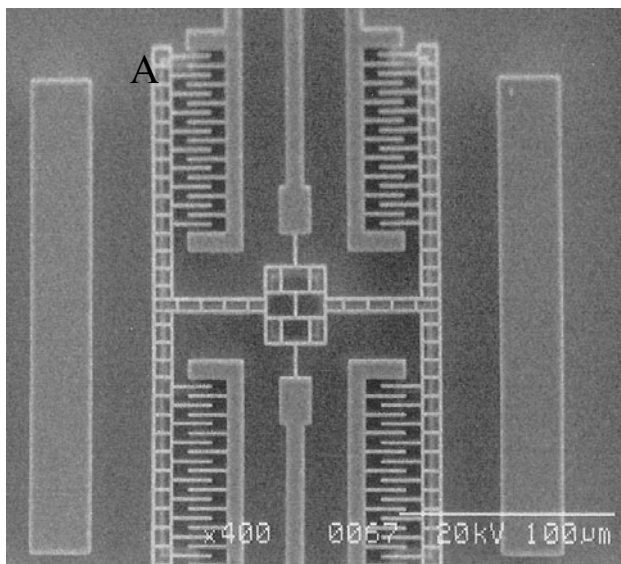


**Figure 1.** Scanning electron micrograph of the oscillator under study. All features including the torsion beam and the comb fingers are  $\sim 1 \mu\text{m}$  wide. The oscillator spans  $\sim 150 \mu\text{m} \times 200 \mu\text{m}$  and is  $\sim 25 \mu\text{m}$  deep.

type' parametric resonance is observed. This two-mode non-degenerate version of parametric amplification offers some advantages over the degenerate version. The driving frequency and the response frequency are decoupled (they are related by integer or fractional harmonics in the case of degenerate amplification). The drive frequency, which is the sum of the first two natural mode frequencies, can be designed to be as far away as needed from the first natural frequency at which the signal gets amplified. This can reduce parasitic coupling between drive and sense. Analysis of coupled parametric systems is discussed in many nonlinear mechanics texts including [13]. Theoretical and experimental studies of the modal interaction in a two degrees of freedom macro mechanical system, which discusses similar resonance effects and the effects of nonlinearity (saturation effects), are discussed in [14].

## 2. Device description

The non-degenerate mode-coupled parametric amplifier/resonator is an electrostatically driven MEM oscillator fabricated with the bulk micromachining process SCREAM [15]. A scanning electron microscope (SEM) image of the device is shown in figure 1. The device has three external bonding pads between which there is electrical isolation. This would allow electrostatic actuation and capacitive detection. In this study, we use electrostatic actuation and optical (laser vibrometry) detection [16] of the out-of-plane motion. However, capacitive detection and comparison with laser vibrometry of similar comb finger architecture has been demonstrated previously, and shown to be a sufficient transduction mechanism for these frequency and amplitude ranges [4]. The first two modes of oscillation for this design are both out-of-plane vibration and are shown in

figure 2. The data presented in figure 2 are experimental results of the mode shapes mapped with the device operating in air using a POLYTEC MSV 300 micro scanning vibrometer.

## 3. Experimental results

A multi-dimensional MEMS motion characterization suite is used to measure the out-of-plane movement of the device [16]. The schematic setup is shown in figure 3. The device is placed in a vacuum chamber, where the pressure is 5 mTorr. The measurements are taken using a laser Doppler vibrometer with built in controllers and sensor heads (Polytec, OFV-3001 and OFV-511) that uses a 633 nm wavelength, 205 mm cavity length helium–neon laser. A voltage source (HP3245A) was used for input voltage signal generation and the displacement and velocity outputs from the vibrometer were recorded and analyzed with a HP spectrum analyzer (HP89470A) and Tektronics oscilloscope (TDS 420 A). The velocity measurements presented in this paper are obtained from the above described setup with measurements taken at one corner of the device (point A in figure 1).

The electrostatic force generated with the out-of-plane electrostatic comb finger configuration is known to be proportional to the square of the applied voltage. Hence, in order to have a single-frequency sinusoidal forcing function with a known dc offset, we use square-rooted sinusoidal voltage signals as our input signal. The frequency response characteristics when driven with 5 V RMS square-rooted sinusoidal input signals near the first two natural frequencies are shown in figures 4(a) and (b). The small RMS value of the input would ensure that no parametric resonance or nonlinearity effects are induced [6]. The natural frequencies can be extracted assuming each mode of the oscillator a forced under-damped SHO. These numbers are only used as a guideline for the testing range of the parametric amplification drive frequencies.

When driven with a square-rooted sinusoidal signal with large amplitude range (20–70 V RMS) at approximately twice the natural frequencies and near the sum of the two natural frequencies, the device is excited at the natural frequencies. Figure 5 shows an experimental map of the areas of parametric excitation. The 'tongues' on the extreme correspond to the two degenerate resonance cases. When driven with an amplitude and frequency corresponding to any point inside these tongues (A and C), the oscillator has a single frequency response at half the drive frequency. For tongue B, the response of the oscillator has two frequency components, such that their sum corresponds to the drive frequency. Figure 6(a) shows a typical time domain response of the oscillator inside the parametric tongue B. Figure 6(b) shows the typical response as a function of the drive frequency near the tongues. Due to a positive cubic nonlinearity, there the response shows bi-stable regions to the right of the tongue [6] for all three areas of parametric resonance.

Parametric mode amplification of the oscillator response can be achieved if, in addition to a direct forcing near the natural frequencies, a pump input signal is added near twice the natural frequency (degenerate mode amplification) or near the sum of the two modes of resonance of the oscillator (non-degenerate mode amplification). This amplification is limited

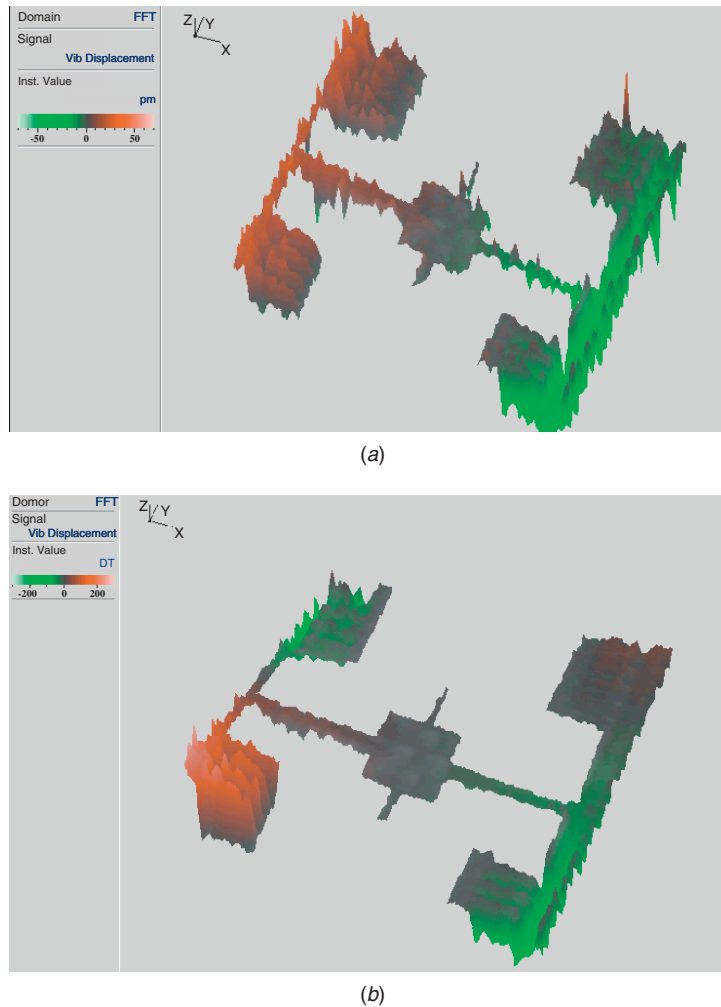


**Figure 2.** The first and second natural modes of the oscillator mapped using a scanning micro vibrometer (Polytec MSV 300). An actuation voltage of 20 V<sub>pk-pk</sub> is used and the device is in air.

(This figure is in colour only in the electronic version)

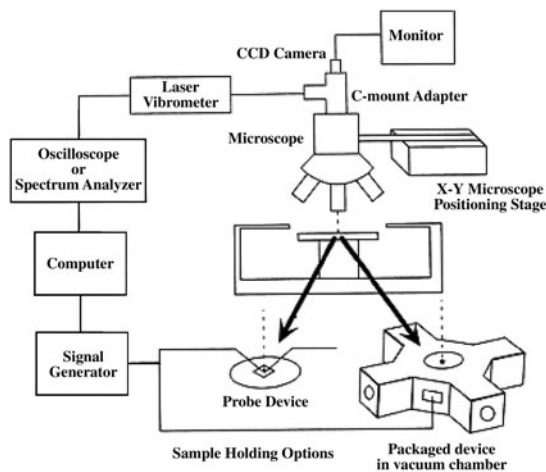


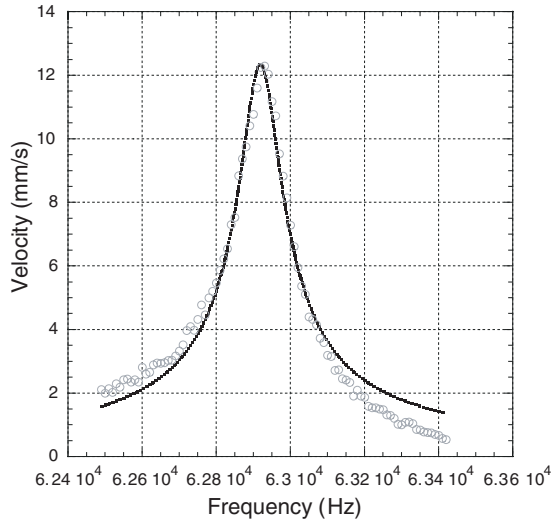
**Figure 3.** Schematic of characterization suite used to test the MEMS oscillator. For the results presented in this paper, we used a vacuum chamber with a pressure of  $\sim 5$  mTorr.

by the nonlinearity in the system or when the system starts to self-oscillate, i.e., is driven inside the tongue region. The gain

defined as the ratio of the oscillator displacement (velocity) with pump-on and with pump-off is plotted for the two modes of the oscillators for degenerate and non-degenerate cases in figure 7. As the amplitude of the direct forcing is increased, the gain saturation occurs at a lower pump amplitude. The angle between the pump signal and the direct drive signal affects the gain in the degenerate case [8] and is maximum when this angle is  $\pm 90^\circ$ . In our experiments, we maintain this angle to be near  $90^\circ$  for both the degenerate cases.

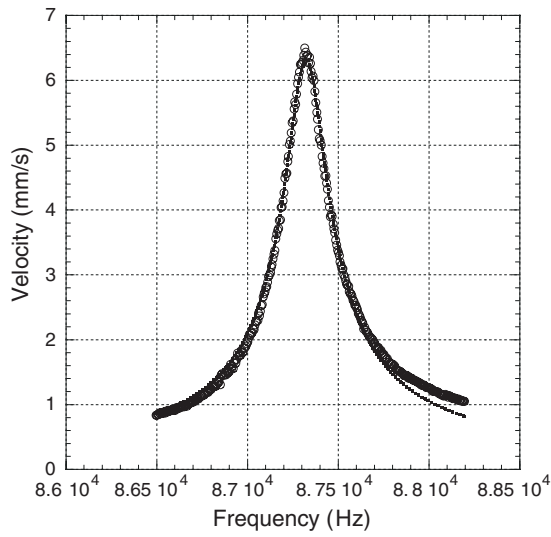
#### 4. Discussion

The experimental verification of the combination type parametric resonance leads to possibilities for enhanced performance in many applications. The non-related drive and output frequencies could simplify detection electronics, reducing parasitic coupling between drive and sense. However, there are issues that need further study and understanding. The exact nature of the mechanical domain and electrostatic nonlinearity plays an important role in degenerate resonance [6]. Hence, it is logical to assume that those factors will play an important role here too.



m1*w/sqrt((1-w*w/(w0*w0))^2+(w/(Q*w0))^2);		
	Value	Error
m1	3.4665e-07	7.0618e-09
w0	62919	1.7143
Q	566.02	18.523
Chisq	25.077	NA
R <sup>2</sup>	0.97325	NA

(a)



m1*w/sqrt((1-w*w/(w0*w0))^2+(w/(Q*w0))^2);		
	Value	Error
m1	1.8863e-07	9.0432e-10
w0	87323	0.7898
Q	384.56	2.9123
Chisq	5.4638	NA
R <sup>2</sup>	0.99322	NA

(b)

**Figure 4.** The frequency response characteristics of the device when driven with a small amplitude voltage signal around the first two modes of the oscillator respectively. The data fit well with the response of a single degree of freedom SHO for each of the modes separately and the fitted parameters are used as a guideline for the locations of the parametric mode resonance regions.

The dynamics can be modeled by coupled Mathieu type equations (equation (1)) to first order. Assuming that the

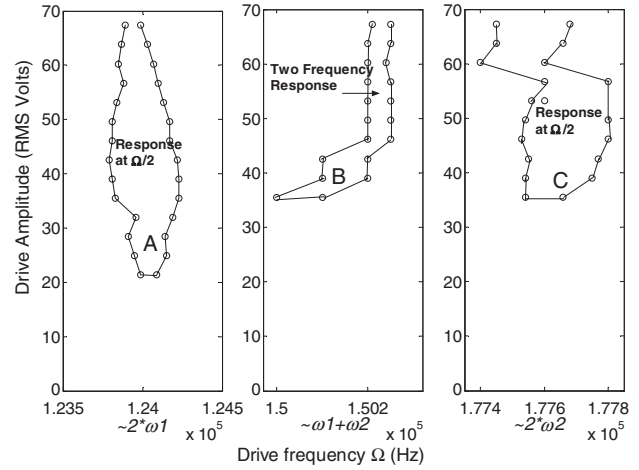


**Figure 5.** Experimental mapping of the regions or ‘tongues’ of parametric resonance. When the drive frequency is nearly twice the natural frequencies, the device has a sub-harmonic response at half the drive frequency. When the drive frequency is nearly the sum of the first two natural frequencies, the device is excited simultaneously in both modes and the response has two frequency components such that their sum is equal to the drive frequency.

‘electrostatic stiffness’ is much smaller than the mechanical stiffness, many methods for the analysis of this equation using perturbations from harmonic response are available in the literature [13]. We have presented details of one such perturbation analysis in the context of two coupled oscillators [11]

The equations of motion can be written as

$$\begin{aligned} \theta_1'' + c_1\theta_1' + (a_1 - 2q_1 \cos 2z)\theta_1 - (2p_1 \cos 2z)\theta_2 + \alpha_1\theta_1^3 &= 0 \\ \theta_2'' + c_2\theta_2' + (a_2 - 2q_2 \cos 2z)\theta_2 - (2p_2 \cos 2z)\theta_1 + \alpha_2\theta_2^3 &= 0 \end{aligned}$$

where

$$\begin{aligned} a_1 &= 4 \frac{(k_{m1} + k_{e1}A)}{I_1\Omega^2}, & c_1 &= 2 \frac{c}{I_1\Omega}, & 2q_1 &= 4 \frac{Ak_{e1}}{I_1\Omega^2}, \\ 2p_1 &= 4 \frac{Ak_{e12}}{I_1\Omega^2}, & \alpha_1 &= 4 \frac{k_{31}}{I_1\Omega^2}, \\ a_2 &= 4 \frac{(k_{m2} + k_{e2}A)}{I_2\Omega^2}, & c_2 &= 2 \frac{c}{I_2\Omega}, & 2q_2 &= 4 \frac{Ak_{e2}}{I_2\Omega^2}, \\ 2p_2 &= 4 \frac{Ak_{e21}}{I_2\Omega^2}, & \alpha_2 &= 4 \frac{k_{32}}{I_2\Omega^2}, \end{aligned} \quad (1)$$

where the electrostatic force when driven with a square-rooted sinusoidal voltage signal has been modeled by  $F_{ei} = k_{ei}V^2\theta_i = k_{ei}A(1 + \cos(\Omega t))\theta_i$  and the equations normalized with respect to time as  $2z = \Omega t$ . The  $k_{mi}$  and  $k_{3i}$  are the mechanical linear and cubic stiffness,  $k_{ei}$  is the ‘electrostatic stiffness’,  $A$  is the squared amplitude of the driving voltage signal,  $\Omega$  is the drive frequency,  $I_i$  is the moment of inertia and  $c$  is a velocity proportional damping constant for each of the modes.

The perturbation analysis using the method of harmonic balance shows the presence of three regions of parametric resonance. Figure 8 shows these regions for non-dimensional

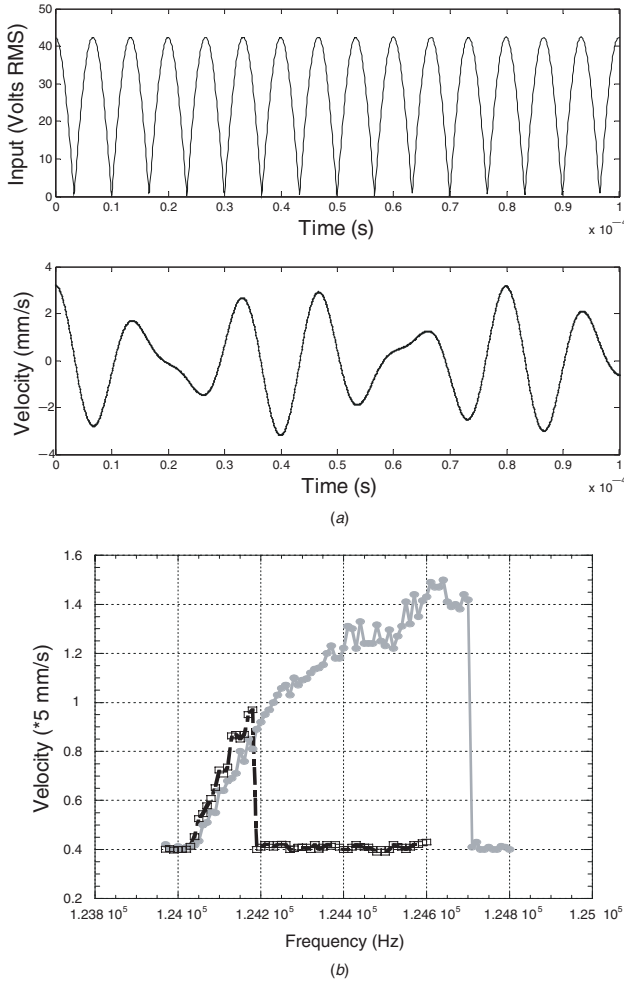


**Figure 6.** (a) Typical input of the voltage signal in the time domain and the time response of the output (velocity) corresponding to the input voltage. The input frequency is close to the sum of the first two natural frequencies, at 150.2 kHz. The output has two distinct frequency components at 62 900 Hz and 87 303 Hz. (b) Typical response amplitude as a function of the quasi-statically varying frequency. These data are for a sweep with an input voltage of 28 V RMS for the degenerate parametric resonance in the first mode. The grey trace is with increasing frequency and the black trace is with decreasing frequency. The effective cubic nonlinearity due to the mechanical and electrostatic effects results in the presence of a bi-stable region. See [6] for a detailed analytical treatment of the effect of cubic nonlinearity.

parameters comparable to those of the device. Note that it compares quite well with the experimentally obtained result in figure 5. For the case of the combined parametric resonance, it appears that the experimentally mapped ‘tongue’ followed on the two ‘dips’ at lower voltages and the other at higher voltage amplitude. The stability of the combination parametric resonance is affected by the phase difference [17] between the modes and is not considered in the current model. The finer features in the experimental result, like the ‘kinks’ (non-smooth lines) in the tongue boundary and narrowing of the boundary with increasing input amplitude (case for the first mode), cannot be explained without taking into account the higher order nonlinearity present in the system. Modeling the rigid body dynamics with nonlinearity effects would be

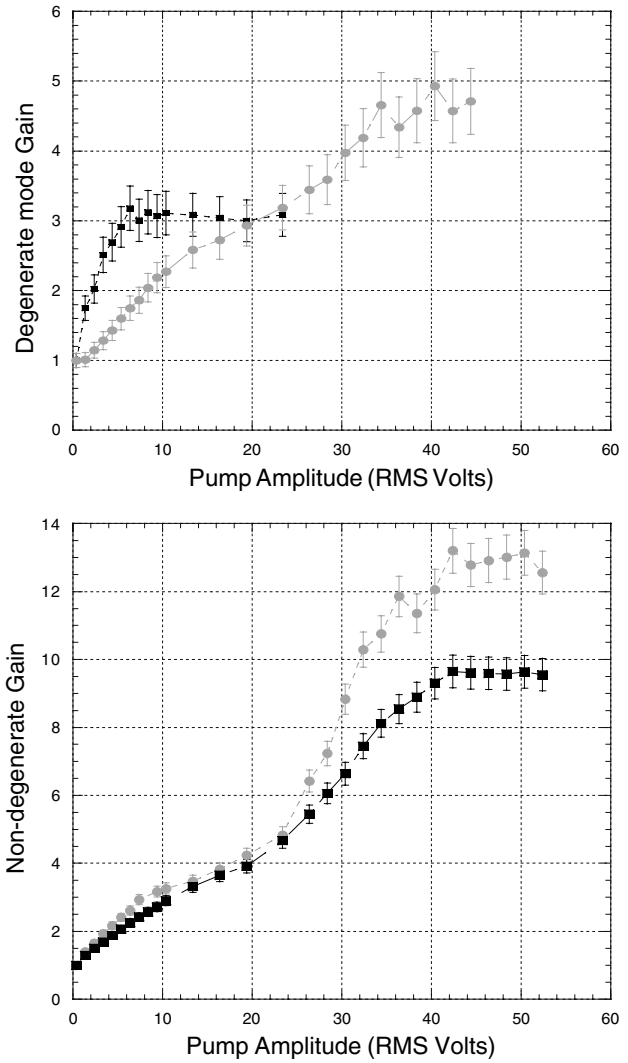


**Figure 7.** The device performance as a parametric amplifier. The black squares are data from the first mode and the grey circles are those from the second mode of oscillation. The plot on the top shows the gain (defined as the output velocity with *pump on*/*pump off*) of the two modes of oscillation as a function of the pump amplitude when pumped with a signal approximately twice the corresponding natural frequency (degenerate parametric amplification). The plot below shows the respective gains of the two modes of response when pumped with the sum of the two modes (non-degenerate parametric amplification). At large pump signals, the gain saturates, as expected, due to self-oscillation and device nonlinearity. The direct driving voltage was 5 V RMS for all these experiments.

useful in designing an optimized amplifier and is in progress now.

The non-degenerate amplification and parametric resonance is possible due to displacement-dependent force generation in either mode of oscillation and due to the interaction between the modes.

The equations of motion of system when the system is being parametrically amplified are

$$\begin{aligned}\theta_1'' + c_1\theta_1' + (a_1 - 2q_1 \cos 2z)\theta_1 - (2p_1 \cos 2z)\theta_2 \\ &= b_{10} + b_1 \sin(z + \phi) \\ \theta_2'' + c_2\theta_2' + (a_2 - 2q_2 \cos 2z)\theta_2 - (2p_2 \cos 2z)\theta_1 \\ &= b_{20} + b_2 \sin(z + \phi)\end{aligned}$$

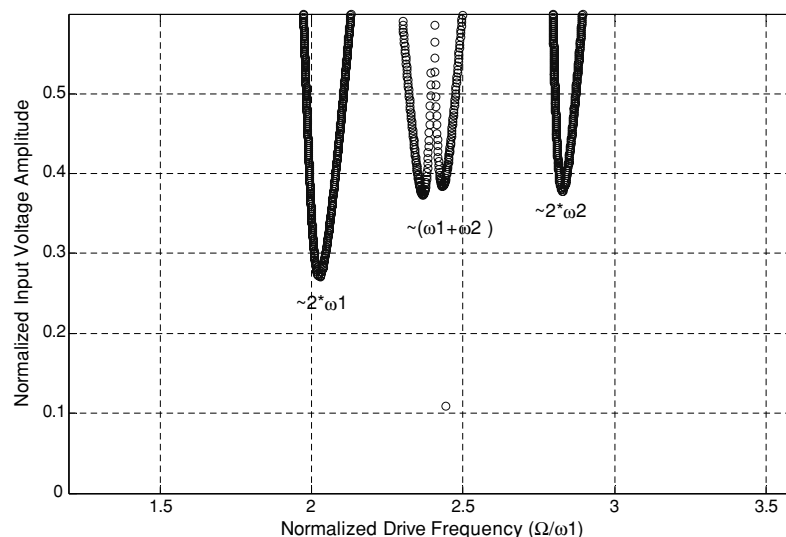


**Figure 8.** Schematic representation of perturbation analysis solution to the coupled Mathieu equation first-order parametric response in applied voltage frequency and amplitude space. In this simulation the electrostatic stiffness has been assumed to be 1/10th of the mechanical stiffness and the non-dimensional damping coefficient to be 0.04. The damping introduces a minimum voltage above which parametric resonance is observed.

where

$$b_{10} = b_1 = 2 \frac{Bk_{e1}}{I_1 \Omega^2} \quad b_{20} = b_2 = 2 \frac{Bk_{e2}}{I_2 \Omega^2} \quad (2)$$

where  $F_{ei} = k_{ei} V^2 \theta_i = k_{ei} A(1 + \cos(\Omega t)) \theta_i$  is a pump force and  $F_i = k_{ei} B(1 + \sin(\Omega t/2 + \phi))$  is a direct driving term.

These conditions are not restricted by device geometry or material system and are satisfied in many common MEMS resonator configurations including simple cantilevers. We have observed similar dynamics in polysilicon cantilever beams [18].

## 5. Conclusion

We have demonstrated non-degenerate parametric resonance and amplification in a torsional MEM oscillator with two interacting mechanical modes of oscillation. The parametric nature arises from time varying stiffness in the system which is in turn caused by displacement-dependent electrostatic force generation in both modes of oscillation. The concept of two-mode parametric amplification and self-resonance in the mechanical domain could be used for signal amplification in various resonant operation micro and nanoscale applications and in mass sensing, communication components such as filters and switches.

## Acknowledgments

The authors would like to thank Eric Lawrence of Polytec PI, Inc., 1342 Bell Ave S-3A Tustin, CA 92780-6440 for mapping the mode shapes using Polytec MSV 300. The work was supported by NSF-CAREER 0093994 and Air Force contract FA9620-02-1-0069.

## References

- [1] Nguyen C T C 1999 Micromechanical filters for miniaturized low-power communications Presented at *Smart Electronics and MEMS (Newport Beach CA, USA, 1999)*
- [2] Dougherty W M, Bruland K J, Garbini J L and Sidles J A 1996 Detection of AC magnetic signals by parametric mode coupling in a mechanical oscillator *Meas. Sci. Technol.* **7** 1733–9
- [3] Chui B W, Kenny T W, Mamin H J, Terris B D and Rugar D 1997 A novel dual-axial AFM cantilever with independent piezoresistive sensors for simultaneous detection of lateral and vertical forces Presented at *1997 ASME Int. Mechanical Engineering Cong. and Exposition, Proc. Symp. on Micro-Mechanical Systems (Dallas, TX, USA)*
- [4] Kenny T 2001 Nanometer-scale force sensing with MEMS devices *IEEE Sensors J.* **1** 148–57
- [5] Louisell W H 1960 *Coupled Mode and Parametric Electronics* (New York: Wiley)
- [6] Zhang W, Baskaran R and Turner K L 2002 Effect of cubic nonlinearity on auto-parametrically amplified resonant MEMS mass sensor *Sensors Actuators A* **102** 139–50
- [7] Dana A, Ho F and Yamamoto Y 1998 Mechanical parametric amplification in piezoresistive gallium arsenide microcantilevers *Appl. Phys. Lett.* **72** 1152–4
- [8] Rugar D and Grutter P 1991 Mechanical parametric amplification and thermomechanical noise squeezing *Phys. Rev. Lett.* **67** 699–702
- [9] Wolfson M B and MacDonald N C 2001 On a MEMS-based parametrically amplified atomic force sensor Presented at *TRANSDUCERS '01. EUROSENSORS XV. 11th Int. Conf. on Solid-State Sensors and Actuators. Digest of Technical Papers (Munich, Germany, 10–14 June 2001)*
- [10] Raskin J P, Brown A R, Khuri-Yakub B and Rebeiz G M 2000 A novel parametric-effect MEMS amplifier *J. Microelectromech. Syst.* **9** 528–37
- [11] Baskaran R and Turner K L 2001 Electrostatic interactions in coupled micro electro mechanical systems Presented at *SPIE's Micro/MEMS (Adelaide, Australia)*
- [12] Olkhovets A, Carr D W, Parpia J M and Craighead H G 2001 Non-degenerate nanomechanical parametric amplifier

- 
- Presented at *Technical Digest. MEMS 2001. 14th IEEE Int. Conf. on Micro Electro Mechanical Systems (Interlaken, Switzerland)*
- [13] Szemplińska-Stupnicka W 1990 *The Behavior of Nonlinear Vibrating Systems* (Dordrecht: Kluwer)
- [14] Haddow A G, Barr A D S and Mook D T 1984 Theoretical and experimental-study of modal interaction in a 2-degree-of-freedom structure *J. Sound Vib.* **97** 451–73
- [15] MacDonald N C 1996 SCREAM microelectromechanical systems *Microelectron. Eng.* **32** 49–73
- [16] Turner K L 1999 Multi-dimensional MEMS motion characterization using laser vibrometry Presented at *Transducers'99. 10th Int. Conf. on Solid-State Sensors and Actuators, Digest of Technical Papers (Sendai, Japan)*
- [17] Bena I and van den Broeck C 1999 Coupled parametric oscillators *Europhys. Lett.* **48** 498–504
- [18] Napoli M, Baskaran R, Turner K and Bameih B 2003 Understanding mechanical domain parametric amplification in micro-cantilevers Presented at *IEEE's MEMS 2003 (Kyoto, Japan)*